

## Flavonoids from *Matteuccia struthiopteris* and Their Anti-influenza Virus (H1N1) Activity

Bo Li,<sup>†,§</sup> Yang Ni,<sup>†</sup> Ling-Juan Zhu,<sup>†</sup> Feng-Bo Wu,<sup>‡</sup> Fei Yan,<sup>†</sup> Xue Zhang,<sup>\*,†,‡</sup> and Xin-Sheng Yao<sup>\*,†,||</sup>

<sup>†</sup>College of Traditional Chinese Materia Medica, Shenyang Pharmaceutical University, Shenyang 110016, People's Republic of China

<sup>‡</sup>State Key Laboratory of Bioactive Substance and Function of Natural Medicines, Institute of Materia Medica, Chinese Academy of Medical Sciences and Peking Union Medical College, Beijing 100050, People's Republic of China

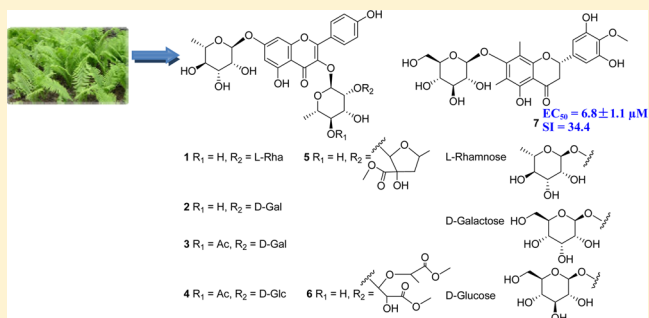
<sup>§</sup>Department of Natural Products Chemistry, College of Pharmacy, China Medical University, Shenyang 110001, People's Republic of China

<sup>‡</sup>Department of Pharmacy, West China Hospital, Sichuan University, Chengdu 610041, People's Republic of China

<sup>||</sup>Institute of Traditional Chinese Medicine & Natural Products, College of Pharmacy, Jinan University, Guangzhou 510632, People's Republic of China

### Supporting Information

**ABSTRACT:** Seven new flavonoid glycosides (1–7), matteflavosides A–G, together with 12 known flavonoids (8–19) were isolated from the rhizomes of *Matteuccia struthiopteris* (L.) Todar. Their structures were established via the analyses of extensive spectroscopic data. All compounds were evaluated for their anti-influenza virus (H1N1) activity using the neuraminidase inhibition assay. The results showed that compound 7 exhibited significant inhibitory activity against the H1N1 influenza virus neuraminidase with an EC<sub>50</sub> value of 6.8 ± 1.1 μM and an SI value of 34.4, and compounds 8 and 17 showed moderate inhibitory activity.

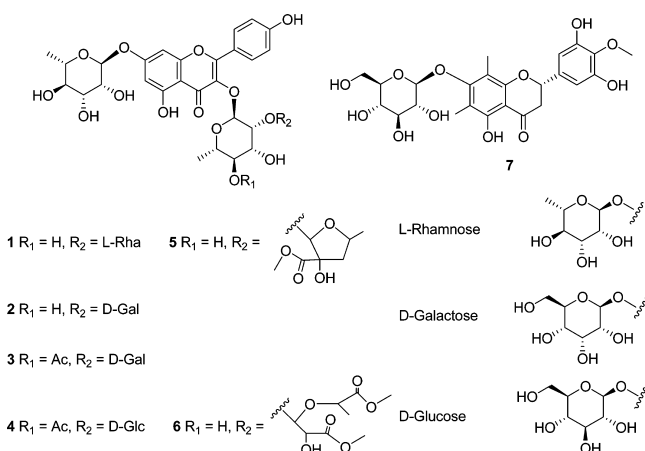


Influenza is an acute respiratory infectious disease caused by the influenza virus. It occurs in annual epidemics, with a peak occurrence during the winter in temperate regions and during rainy seasons in some tropical countries, resulting in significant morbidity and mortality.<sup>1</sup> The influenza virus is a member of the Orthomyxoviridae family, which is divided into types A, B, and C based on the antigenicity of the nucleoprotein (NP) and matrix protein (M1). Type A is primarily responsible for annual epidemics or pandemic outbreaks.<sup>2</sup> It is widely accepted that vaccination remains the most effective approach for the prevention of the viral infections, but the development of vaccines is a relatively hysteric process because of the high mutation rate of the virus. Therefore, anti-influenza drugs play a critical role in the prevention and management of influenza infections. Currently, there are two classes of drugs licensed for influenza infections in humans: the M2 ion channel blockers amantadine and rimantadine, and the neuraminidase (NA) inhibitors oseltamivir, zanamivir, and peramivir.<sup>3,4</sup> However, problems regarding these drugs have been reported due to adverse effects, risk of emergence of resistant viruses, loss of efficacy due to serotype variation, and, for the adamantanes, lack of activity against influenza B.<sup>5–8</sup> As a result, the discovery process for new anti-influenza drugs has resulted in much attention being paid to natural products as sources of new antiviral compounds with high efficiency and low toxicity.

*Matteuccia struthiopteris* (L.) Todar (Onocleaceae) is widely distributed in the temperate regions of the northern hemisphere and has been used as both a health food in many countries and a traditional medicine in China since ancient times.<sup>9–12</sup> The rhizomes of *M. struthiopteris*, possessing flavonoids, phenolics, stilbenes, and steroids,<sup>11,13–16</sup> are used as traditional Chinese and folk remedies for the treatment of pinworm, enterozoic abdominalgia, dysentery, hematochezia and metrorrhagia, and prevention of influenza, Japanese encephalitis, and viral parotitis.<sup>10</sup> These traditional uses suggest that this plant may contain compounds with anti-influenza virus activities. Therefore, systematic studies of the chemical constituents of the rhizomes of *M. struthiopteris* and their anti-influenza virus (H1N1) activity have been carried out. Seven new flavonoid glycosides (1–7), matteflavosides A–G, together with 12 known flavonoids (8–19) were isolated from the 60% EtOH extract of the rhizomes of *M. struthiopteris*. In the neuraminidase inhibition assay, compound 7 exhibited potent antiviral activity against the influenza A (H1N1) virus, and compounds 8 and 17 showed moderate inhibitory activity. No previous investigations regarding the anti-influenza virus activity of the constituents isolated from the genus *Matteuccia* have been reported. In this paper, the isolation, structural

Received: November 6, 2014

characterization, and anti-influenza virus (H1N1) activity of the isolated flavonoids are described.



## RESULTS AND DISCUSSION

Matteflavoside A (**1**) was obtained from the 60% EtOH extract of the rhizomes of *M. struthiopteris* as a yellowish, amorphous powder,  $[\alpha]_D^{25} -13.4$  (*c* 0.5, MeOH). The UV absorption maxima of **1** were at 266 and 346 nm, characteristic of a 3-substituted flavonol. The IR spectrum showed absorption bands for the hydroxy group(s) ( $3427\text{ cm}^{-1}$ ), carbonyl group(s) ( $1655\text{ cm}^{-1}$ ), and aromatic ring(s) ( $1602$ ,  $1492$ , and  $1450\text{ cm}^{-1}$ ). Its molecular formula was deduced as  $C_{33}H_{40}O_{18}$  by  $^{13}C$  NMR data and HRESIMS, giving a quasimolecular ion peak  $[M + H]^+$  at  $m/z$  725.2296 (calcd 725.2293). In addition, the HRESIMS spectra of compound **1** showed fragment ions at  $m/z$  579.1721  $[M + H - C_6H_{10}O_4]^+$ , 433.1134  $[M + H - 2 \times C_6H_{10}O_4]^+$ , and 287.0554  $[M + H - 3 \times C_6H_{10}O_4]^+$ , suggesting that there were three deoxyhexose units in **1**. The acid hydrolysis and high-performance liquid chromatography (HPLC) analysis,<sup>17</sup> in combination with the  $^{13}C$  NMR data, confirmed the presence of  $\alpha$ -L-rhamnose. The

$^1H$  NMR spectrum of **1** exhibited resonances for *meta*-coupled aromatic protons at  $\delta_H$  6.46 and 6.78 (each 1H, d,  $J = 2.0$  Hz) in ring A, an AA'XX' coupling system at  $\delta_H$  7.83 and 6.95 (each 2H, d,  $J = 8.8$  Hz) in ring B, and two phenolic hydroxy groups at  $\delta_H$  12.67 and 10.27 (each 1H, s). Based on the above evidence, the aglycone of **1** was identified as kaempferol. The proton signals at  $\delta_H$  5.50 (1H, br s)/0.89 (3H, d,  $J = 6.4$  Hz), 4.12 (1H, m)/0.98 (3H, d,  $J = 6.4$  Hz), and 5.55 (1H, br s)/1.12 (3H, d,  $J = 6.0$  Hz) were attributed to three rhamnosyl moieties in the  $^1H$  NMR spectrum of **1**. Two of these rhamnosyl moieties were linked to the aglycone at C-3 and C-7, as indicated by the HMBC correlations (Figure 1) of H-1''/C-3 and H-1'''/C-7, respectively. The HMBC correlations of H-1'''/C-2'' and H-2''/C-1''' established that the remaining rhamnosyl unit was attached to C-2'' of the C-3 rhamnosyl moiety. On the basis of the above evidence, the structure of compound **1** was determined to be kaempferol-3-O-[ $\alpha$ -L-rhamnopyranosyl-(1 $\rightarrow$ 2)- $\alpha$ -L-rhamnopyranosyl]-7-O- $\alpha$ -L-rhamnopyranoside.

Matteflavoside B (**2**) was isolated as a yellowish, amorphous powder,  $[\alpha]_D^{25} -30.4$  (*c* 0.5, MeOH). The molecular formula  $C_{33}H_{40}O_{19}$  was determined by  $^{13}C$  NMR data and HRESIMS ion at  $m/z$  741.2242  $[M + H]^+$  (calcd 741.2242). In addition, the HRESIMS spectra of compound **2** showed fragment ions at  $m/z$  579.1714  $[M + H - C_6H_{10}O_5]^+$ , 433.1136  $[M + H - C_6H_{10}O_5 - C_6H_{10}O_4]^+$ , and 287.0558  $[M + H - C_6H_{10}O_5 - 2 \times C_6H_{10}O_4]^+$ , suggesting that there were two deoxyhexose and one hexose unit in **2**. The acid hydrolysis and HPLC analysis,<sup>17</sup> in combination with the  $^{13}C$  NMR data and the coupling constant of the anomeric proton (H-1''', 6.8 Hz), confirmed the presence of  $\alpha$ -L-rhamnose and  $\beta$ -D-galactose. Compound **2** displayed UV maximal absorptions and IR absorption bands similar to those of **1**. The  $^1H$  and  $^{13}C$  NMR spectra of **2** (Tables 1 and 2) were also similar to those of **1**. The differences involved the substitution of a galactosyl unit at C-2'' of the C-3 rhamnosyl moiety instead of a rhamnosyl unit, according to the HMBC correlation between the anomeric proton of galactose at  $\delta_H$  4.19 (H-1''') and C-2''. Thus, the structure of compound

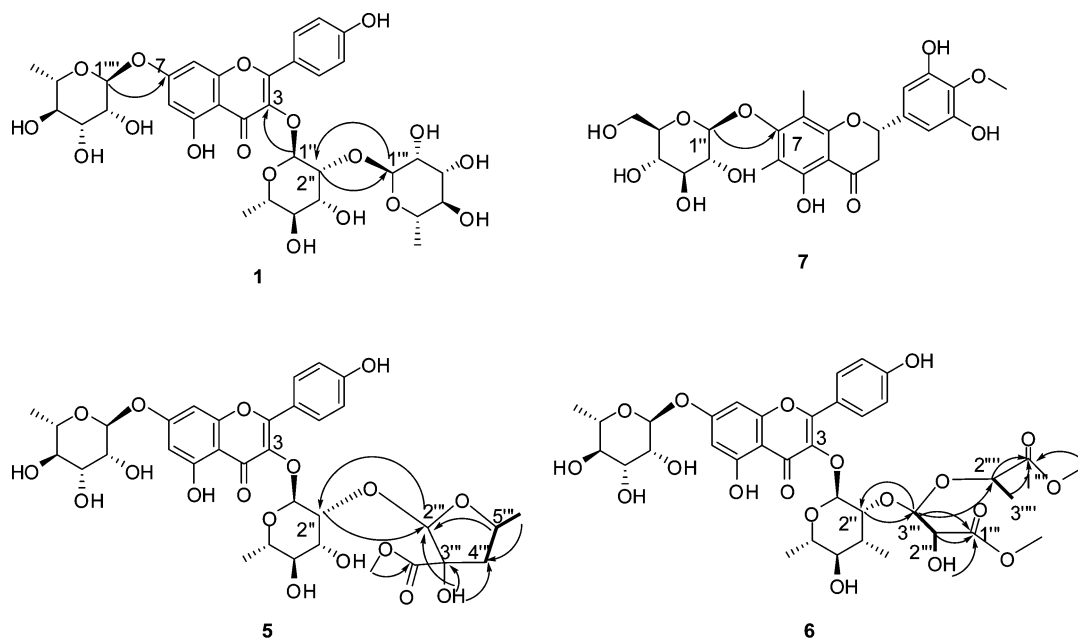


Figure 1. Key HMBC (arrows) and  $^1H$ - $^1H$  COSY (bold lines) correlations of compounds **1** and **5**-**7**.

Table 1. <sup>1</sup>H NMR Spectroscopic Data (DMSO-*d*<sub>6</sub>) for Compounds 1–7 (J in Hz)

position	1 <sup>a</sup>	2 <sup>a</sup>	3 <sup>a</sup>	4 <sup>a</sup>	5 <sup>b</sup>	6 <sup>a</sup>	7 <sup>a</sup>
2							5.40 dd (12.0, 2.8)
3							3.14 m
6	6.46 d (2.0)	6.46 d (2.0)	6.46 d (2.0)	6.46 d (2.0)	6.46 d (2.4)	6.47 d (2.0)	
8	6.78 d (2.0)	6.78 d (2.0)	6.78 d (2.0)	6.79 d (2.0)	6.78 d (2.4)	6.80 d (2.0)	
2'/6'	7.83 d (8.8)	7.80 d (8.4)	7.78 d (8.4)	7.81 d (8.8)	7.79 d (9.0)	7.79 d (8.8)	6.46 s
3'/5'	6.95 d (8.8)	6.94 d (8.4)	6.97 d (8.4)	6.96 d (8.8)	6.92 d (9.0)	6.93 d (8.8)	
6-CH <sub>3</sub>							2.08 s
8-CH <sub>3</sub>							2.09 s
4'-OCH <sub>3</sub>							3.68 s
4'-OH	10.27 s	10.26 s	10.31 s	10.29 s	10.30 s	10.27 s	
5-OH	12.67 s	12.57 s	12.52 s	12.49 s	12.65 s	12.50 s	12.08 s
3'/5'-OH							9.20 s
(3-O-Rha)1 <sup>n</sup>	5.50 br s	5.61 br s	5.65 br s	5.60 br s	5.38 br s	5.39 d (1.2)	(7-O-Glc) 4.59 d (7.2)
2 <sup>n</sup>	4.01 d (2.4)	4.02 m	4.06 d (2.8)	4.15 d (2.8)	4.10 m	4.32 m	3.30 m
3 <sup>n</sup>	3.54–3.58 <sup>c</sup>	3.52–3.54 <sup>c</sup>	3.75 br s	3.78 br s	3.56–3.60 <sup>c</sup>	3.58–3.62 <sup>c</sup>	3.24 m
4 <sup>n</sup>	3.13 br s	3.13 m	4.64 t (10.0)	4.65 d (10.0)	2.96 m	3.17 m	3.10–3.14 <sup>c</sup>
5 <sup>n</sup>	3.42–3.48 <sup>c</sup>	3.22 m	3.38–3.42 <sup>c</sup>	3.58 dd (6.0, 10.0)	3.12–3.16 <sup>c</sup>	3.23 m	3.07 m
6 <sup>n</sup>	0.89 d (6.4)	0.86 d (6.0)	0.76 d (6.4)	0.78 d (6.0)	0.81 d (6.0)	0.85 d (6.0)	3.40–3.44, <sup>c</sup> 3.62 m
4 <sup>n</sup> -COCH <sub>3</sub>			2.02 s	2.04 s			
1 <sup>m</sup>	4.12 m	4.19 d (6.8)	4.14 d (7.6)	4.21 d (8.0)			
2 <sup>m</sup>	3.26–3.30 <sup>c</sup>	3.30–3.33 <sup>c</sup>	3.30–3.33 <sup>c</sup>	3.02 m	5.13 s	4.02 t (6.0)	
3 <sup>m</sup>	3.26–3.30 <sup>c</sup>	3.30–3.33 <sup>c</sup>	3.30–3.33 <sup>c</sup>	3.12–3.16 <sup>c</sup>		4.88 d (6.0)	
4 <sup>m</sup>	3.35–3.40 <sup>c</sup>	3.64 m	3.64 m	3.12–3.16 <sup>c</sup>	1.98 m		
5 <sup>m</sup>	3.35–3.40 <sup>c</sup>	3.30–3.33 <sup>c</sup>	3.26 br s	2.97 br s	4.26 m		
6 <sup>m</sup>	0.98 d (6.4)	3.39 m, 3.47 m	3.37 m, 3.47 m	3.41 m			
1 <sup>m</sup> -OCH <sub>3</sub>						3.64 s	
3 <sup>m</sup> -COOCH <sub>3</sub>					3.61 s		
3 <sup>m</sup> -OH					5.99 s	6.08 d (6.0)	
5 <sup>m</sup> -CH <sub>3</sub>					1.12 d (6.0)		
1 <sup>m</sup>	5.55 br s						
2 <sup>m</sup>	3.84 s	3.83 m	3.84 br s	3.85 br s	3.83 br s	4.53 q (6.8)	
3 <sup>m</sup>	3.62 m	3.64 m	3.64 br s	3.64 dd (3.2, 9.2)	3.63 m	1.26 d (6.8)	
4 <sup>m</sup>	3.26–3.30 <sup>c</sup>	3.27–3.31 <sup>c</sup>	3.28–3.33 <sup>c</sup>	3.28–3.32 <sup>c</sup>	3.28–3.32 <sup>c</sup>		
5 <sup>m</sup>	3.40–3.45 <sup>c</sup>						
6 <sup>m</sup>	1.12 d (6.0)	1.13 d (6.4)	1.13 d (6.0)	1.13 d (6.0)	1.12 d (6.0)		
1 <sup>m</sup> -OCH <sub>3</sub>						3.64 s	
1 <sup>m</sup>						5.56 br s	
2 <sup>m</sup>						3.84 m	
3 <sup>m</sup>						3.61 m	
4 <sup>m</sup>						3.26–3.30 <sup>c</sup>	
5 <sup>m</sup>						3.43 m	
6 <sup>m</sup>						1.13 d (6.0)	

<sup>a</sup>Measured at 400 MHz. <sup>b</sup>Measured at 600 MHz. <sup>c</sup>Signals overlapped.

2 was established as kaempferol-3-*O*-[ $\beta$ -D-galactosyl-(1 $\rightarrow$ 2)- $\alpha$ -L-rhamnopyranosyl]-7-*O*- $\alpha$ -L-rhamnopyranoside.

Matteflavoside C (3), a yellowish, amorphous powder, [ $\alpha$ ]<sub>D</sub><sup>25</sup> –70.4 (c 0.5, MeOH), gave a molecular formula of C<sub>35</sub>H<sub>42</sub>O<sub>20</sub> by <sup>13</sup>C NMR data and HRESIMS (783.2366, [M + H]<sup>+</sup>). The <sup>1</sup>H and <sup>13</sup>C NMR data (Tables 1 and 2) for 3 were similar to those for 2, except for the presence of an acetyl group. The HMBC correlation between H-4<sup>n</sup> and the carbonyl carbon of the acetyl group at  $\delta$ <sub>C</sub> 169.8 indicated the acetylation of 4<sup>n</sup>-OH of the C-3 rhamnosyl moiety. Therefore, the structure of 3 was elucidated as kaempferol-3-*O*-[ $\beta$ -D-galactopyranosyl-(1 $\rightarrow$ 2)-4-*O*-acetyl- $\alpha$ -L-rhamnopyranosyl]-7-*O*- $\alpha$ -L-rhamnopyranoside.

Matteflavoside D (4) was obtained as a yellowish, amorphous powder, [ $\alpha$ ]<sub>D</sub><sup>25</sup> –25.2 (c 0.5, MeOH). Its molecular formula was established as C<sub>35</sub>H<sub>42</sub>O<sub>20</sub> by <sup>13</sup>C NMR data and HRESIMS ion at *m/z* 783.2345 [M + H]<sup>+</sup> (calcd 783.2348), in agreement

with that of 3. The <sup>1</sup>H and <sup>13</sup>C NMR data (Tables 1 and 2) for 4 were similar to those of 3, except for a D-glucosyl unit replacing the D-galactosyl unit, which was supported by the result of the acid hydrolysis and HPLC analysis.<sup>17</sup> The HMBC correlation between the anomeric proton of glucose at  $\delta$ <sub>H</sub> 4.21 (H-1<sup>m</sup>) and C-2<sup>n</sup> further confirmed the above conclusion. The  $\beta$ -configuration of the glucosyl moiety was assigned from the large coupling constant (8.0 Hz) of the anomeric proton. Based on the above evidence, the structure of compound 4 was deduced as kaempferol-3-*O*-[ $\beta$ -D-glucopyranosyl-(1 $\rightarrow$ 2)-4-*O*-acetyl- $\alpha$ -L-rhamnopyranosyl]-7-*O*- $\alpha$ -L-rhamnopyranoside.

Matteflavoside E (5) was a yellowish, amorphous powder, [ $\alpha$ ]<sub>D</sub><sup>25</sup> –79.2 (c 0.5, MeOH). The HRESIMS showed a quasimolecular ion peak at *m/z* 737.2292 [M + H]<sup>+</sup> (calcd 737.2293), indicating a molecular formula of C<sub>34</sub>H<sub>40</sub>O<sub>18</sub>, which was consistent with the <sup>13</sup>C NMR data. The <sup>1</sup>H and <sup>13</sup>C NMR

Table 2.  $^{13}\text{C}$  NMR Spectroscopic Data (DMSO- $d_6$ ) for Compounds 1–7

position	1 <sup>a</sup>	2 <sup>a</sup>	3 <sup>a</sup>	4 <sup>a</sup>	5 <sup>b</sup>	6 <sup>a</sup>	7 <sup>a</sup>
2	157.5 C	157.6 C	157.9 C	157.7 C	157.8 C	157.7 C	77.7 CH
3	134.8 C	134.5 C	134.3 C	134.6 C	134.4 C	134.8 C	42.4 CH <sub>2</sub>
4	177.9 C	177.8 C	177.6 C	177.7 C	177.9 C	177.8 C	198.1 C
5	160.9 C	160.9 C	160.9 C	160.8 C	161.0 C	160.8 C	157.8 C
6	99.4 CH	99.4 CH	99.4 CH	99.4 CH	99.5 CH	99.4 CH	111.2 C
7	161.7 C	161.4 C					
8	94.6 CH	110.0 C					
9	156.0 C	156.0 C	156.1 C	156.0 C	156.1 C	156.1 C	157.1 C
10	105.6 C	105.7 C	104.8 C				
1'	120.2 C	120.2 C	120.0 C	120.0 C	120.2 C	120.1 C	134.0 C
2', 6'	130.6 CH	130.6 CH	130.6 CH	130.6 CH	130.7 CH	130.6 CH	105.4 CH
3', 5'	115.5 CH	115.4 CH	115.4 CH	115.4 CH	115.5 CH	115.3 CH	150.7 C
4'	160.3 C	160.2 C	160.3 C	160.3 C	160.3 C	160.2 C	135.4 C
6-CH <sub>3</sub>							8.6 CH <sub>3</sub>
8-CH <sub>3</sub>							9.2 CH <sub>3</sub>
4'-OCH <sub>3</sub>							59.6 CH <sub>3</sub>
(3-O-Rha)1''	101.1 CH	100.7 CH	100.2 CH	100.5 CH	100.5 CH	100.7 CH	(7-O-Glc) 104.1 CH
2''	81.3 CH	80.9 CH	80.7 CH	80.9 CH	74.9 CH	78.5 CH	74.0 CH
3''	70.1 CH	70.1 CH	67.5 CH	67.5 CH	69.9 CH	70.0 CH	76.3 CH
4''	71.7 CH	71.7 CH	73.4 CH	73.3 CH	71.3 CH	71.1 CH	69.9 CH
5''	70.2 CH	70.4 CH	67.4 CH	67.4 CH	70.6 CH	70.6 CH	77.0 CH
6''	17.3 CH <sub>3</sub>	17.3 CH <sub>3</sub>	16.9 CH <sub>3</sub>	16.9 CH <sub>3</sub>	17.7 CH <sub>3</sub>	17.2 CH <sub>3</sub>	61.0 CH <sub>2</sub>
4''-CO			169.8 C	169.8 C			
4''-COCH <sub>3</sub>			20.7 CH <sub>3</sub>	20.7 CH <sub>3</sub>			
1'''	106.6 CH	106.5 CH	106.6 CH	106.1 CH		170.7 C	
2'''	70.9 CH	71.1 CH	70.8 CH	73.6 CH	107.2 C	72.9 CH	
3'''	73.1 CH	73.0 CH	72.9 CH	76.1 CH	83.7 C	103.4 CH	
4'''	70.4 CH	67.6 CH	67.5 CH	69.1 CH	39.9 CH <sub>2</sub>		
5'''	70.7 CH	74.9 CH	74.9 CH	76.6 CH	75.2 CH		
6'''	16.2 CH <sub>3</sub>	59.7 CH <sub>2</sub>	59.6 CH <sub>2</sub>	60.3 CH <sub>2</sub>			
1'''-OCH <sub>3</sub>						51.6 CH <sub>3</sub>	
3'''-CO					171.0 C		
3'''-COOCH <sub>3</sub>					51.6 CH <sub>3</sub>		
5'''-CH <sub>3</sub>					22.6 CH <sub>3</sub>		
1''''	98.5 CH	98.4 CH	98.4 CH	98.4 CH	98.4 CH	172.0 C	
2''''	69.8 CH	69.8 CH	69.7 CH	69.7 CH	69.8 CH	71.1 CH	
3''''	70.2 CH	18.4 CH <sub>3</sub>					
4''''	71.6 CH	71.6 CH	71.5 CH	71.5 CH	71.5 CH		
5''''	70.0 CH	70.0 CH	70.0 CH	70.0 CH	70.1 CH		
6''''	17.8 CH <sub>3</sub>	17.8 CH <sub>3</sub>	17.8 CH <sub>3</sub>	17.8 CH <sub>3</sub>	17.9 CH <sub>3</sub>		
1''''-OCH <sub>3</sub>						51.3 CH <sub>3</sub>	
1'''''						98.4 CH	
2'''''						69.7 CH	
3'''''						70.2 CH	
4'''''						71.5 CH	
5'''''						70.0 CH	
6'''''						17.8 CH <sub>3</sub>	

<sup>a</sup>Measured at 100 MHz. <sup>b</sup>Measured at 150 MHz.

data (Tables 1 and 2) for **5** were similar to those for **1**, except for the absence of the rhamnosyl moiety. In addition, the  $^1\text{H}$  and  $^{13}\text{C}$  NMR spectra of **5** exhibited one carbonyl, one acetal group, one oxygenated tertiary carbon, one oxygenated methine, one methylene, one methyl, one methoxy group, and one hydroxy group. The  $^1\text{H}$ – $^1\text{H}$  COSY correlations between H-5''' and H-4''', 5'''-CH<sub>3</sub> and HMBC correlations for 3'''-OH/C-2''', C-3''', C-4''', H-2'''/C-4''', C-5''', and H-4'''/C-2''', C-3''' (Figure 1), in combination with the molecular formula and index of hydrogen deficiency, revealed the presence of a tetrahydrofuran ring fragment with a hydroxy

group at C-3''' and a methyl group located at C-5'''. Additionally, the correlation between –OCH<sub>3</sub> ( $\delta_{\text{H}}$  3.61) and the carbon at  $\delta_{\text{C}}$  171.0 in the HMBC spectrum of **5** indicated the presence of a –COOCH<sub>3</sub> group attached to C-3'''. The above tetrahydrofuran ring fragment was linked to C-2''' of the C-3 rhamnosyl moiety through an oxygen atom, as indicated by the correlations of H-2'''/C-2''' and H-2'''/C-2''' in the HMBC spectrum. The NOESY spectrum of **5** showed the correlations for 3'''-OH/H-2''', H-5''', and 3'''-COOCH<sub>3</sub>/5'''-CH<sub>3</sub> (Figure 2), suggesting that the relative configuration of the tetrahydrofuran ring was 2'''S\*3'''R\*5'''R\* or 2'''R\*3'''S\*5'''S\*. On the

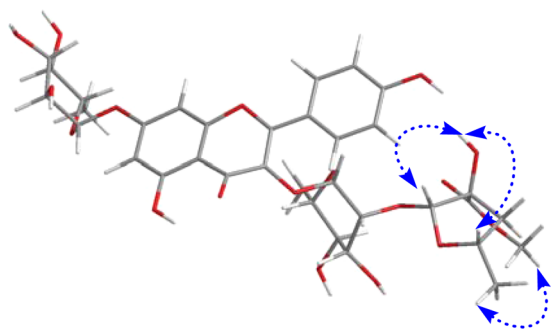


Figure 2. Key NOESY (arrows) correlations of compound 5.

basis of the above evidence, the structure of compound 5 was determined to be kaempferol-3-*O*-[(2,3-dihydroxy-3-methoxycarbonyl-5-methyltetrahydrofuran-2-yl)-(2→2)- $\alpha$ -L-rhamnopyranosyl]-7-*O*- $\alpha$ -L-rhamnopyranoside.

Matteflavoside F (6) was obtained as a yellowish, amorphous powder,  $[\alpha]_D^{25} -8.4$  (*c* 0.5, MeOH). The  $^{13}\text{C}$  NMR data and HRESIMS (783.2351  $[\text{M} + \text{H}]^+$ ) revealed the molecular formula as  $\text{C}_{35}\text{H}_{42}\text{O}_{20}$ . In the  $^1\text{H}$  and  $^{13}\text{C}$  NMR spectra, the differences between 6 and 1 were the absence of a rhamnopyranosyl moiety and the presence of two carbonyls, one acetal group, two oxygenated methines, one methyl, two methoxy groups, and one hydroxy group. The  $^1\text{H}$ - $^1\text{H}$  COSY correlations at H-2'''/H-3''', 2'''-OH, and H-2'''/H-3''' and the HMBC correlations for H-3'''/C-2''' (Figure 1) indicated the presence of a fragment  $\text{CH}_3\text{CHOCH}(\text{O})\text{CH}(\text{OH})-$ . Additionally, the correlations between  $-\text{OCH}_3$  ( $\delta_{\text{H}}$  3.64) and the carbons at  $\delta_{\text{C}}$  170.7 and 172.0 in the HMBC spectrum of 6 showed the presence of two  $-\text{COOCH}_3$  fragments, one of which was linked to C-2''', in accordance with the HMBC correlations of H-2''' and H-3'''/C-1'''. The second  $-\text{COOCH}_3$  fragment was attached to C-2''', in accordance with the correlations of 2'''-OH, H-2''', and H-3'''/C-1'''. The above six-carbon chain was attached to C-2''' of the C-3 rhamnopyranosyl moiety, according to the correlation between H-3''' and C-2''' in the HMBC spectrum. Based on the above evidence, the structure of compound 6 was established as kaempferol-3-*O*-{methyl 2,3-dihydroxy-3-[(1-methoxy-1-oxopropan-2-yl)oxy]propanoate-(3→2)- $\alpha$ -L-rhamnopyranosyl}-7-*O*- $\alpha$ -L-rhamnopyranoside.

Matteflavoside G (7), a yellowish amorphous powder,  $[\alpha]_D^{25} -4.0$  (*c* 0.5, MeOH), had a molecular formula of  $\text{C}_{24}\text{H}_{28}\text{O}_{12}$  on the basis of  $^{13}\text{C}$  NMR data and HRESIMS at  $m/z$  509.1661  $[\text{M} + \text{H}]^+$  (calcd 509.1659). The IR spectrum showed absorption bands for hydroxy ( $3442\text{ cm}^{-1}$ ) and carbonyl ( $1633\text{ cm}^{-1}$ ) groups and aromatic ring(s) ( $1601$ ,  $1515$ , and  $1442\text{ cm}^{-1}$ ). The UV absorption maxima of 7 were at 283 and 357 nm, suggesting the presence of a flavanone skeleton in the structure. The  $^1\text{H}$  and  $^{13}\text{C}$  NMR spectra of 7 were similar to those of the known flavanone ophiofolius A (17),<sup>18</sup> except for the presence of a sugar moiety. Acid hydrolysis followed by HPLC analysis using an authentic sample as reference<sup>17</sup> confirmed the presence of D-glucose. Additionally, the configuration of the anomeric carbon was deduced to be  $\beta$  based on the coupling constant of the anomeric proton (7.2 Hz). The glucosidic linkage was established by the HMBC correlation (Figure 1) between H-1'' ( $\delta_{\text{H}}$  4.59) and C-7, indicating that the glucosyl moiety was attached to C-7. The electronic circular dichroism (ECD) spectrum of 7 showed a negative Cotton effect at 283 nm and a positive Cotton effect at 354 nm, suggesting that the absolute configuration at C-2 was *S*.<sup>19</sup> Therefore, the structure of 7 was identified as (2*S*)-6,8-dimethyl-4'-methoxy-5,3',5'-trihydroxyflavanone-7-*O*- $\beta$ -D-glucopyranoside.

Additionally, 12 known compounds were isolated and identified as kaempferol-3-*O*- $\beta$ -D-glucopyranoside (8),<sup>20</sup> kaempferol-3-*O*- $\beta$ -D-glucopyranosyl-7-*O*- $\alpha$ -L-rhamnopyranoside (9),<sup>21</sup> kaempferol-3,7-di-*O*- $\alpha$ -L-rhamnopyranoside (10),<sup>22</sup> kaempferol-3-*O*-( $\alpha$ -L-3-*O*-acetyl-rhamnopyranosyl)-7-*O*- $\alpha$ -L-rhamnopyranoside (11),<sup>23</sup> kaempferol-3-*O*-( $\alpha$ -L-2-*O*-acetyl-rhamnopyranosyl)-7-*O*- $\alpha$ -L-rhamnopyranoside (12),<sup>24</sup> kaempferol-3-*O*-( $\alpha$ -L-4-*O*-acetyl-rhamnopyranosyl)-7-*O*- $\alpha$ -L-rhamnopyranoside (13),<sup>25</sup> kaempferol-3-*O*-[ $\beta$ -D-glucopyranosyl-(1→2)- $\alpha$ -L-rhamnopyranosyl]-7-*O*- $\alpha$ -L-rhamnopyranoside (14),<sup>26</sup> kaempferol-3-*O*-[1,2,4-trihydroxy-3-oxo-5-methyltetrahydropyran-(1→2)- $\alpha$ -L-rhamnopyranosyl]-7-*O*- $\alpha$ -L-rhamnopyranoside (15),<sup>27</sup> protoapigenone (16),<sup>28</sup> ophiofolius A (17),<sup>18</sup> apigenin-4'-*O*- $\beta$ -D-glucopyranoside (18),<sup>29</sup> and matteorien (19)<sup>30</sup> by comparison of observed and published data. Compounds 8–18 are reported from the *Matteuccia* genus for the first time, and compound 19 has not been previously reported to come from this plant.

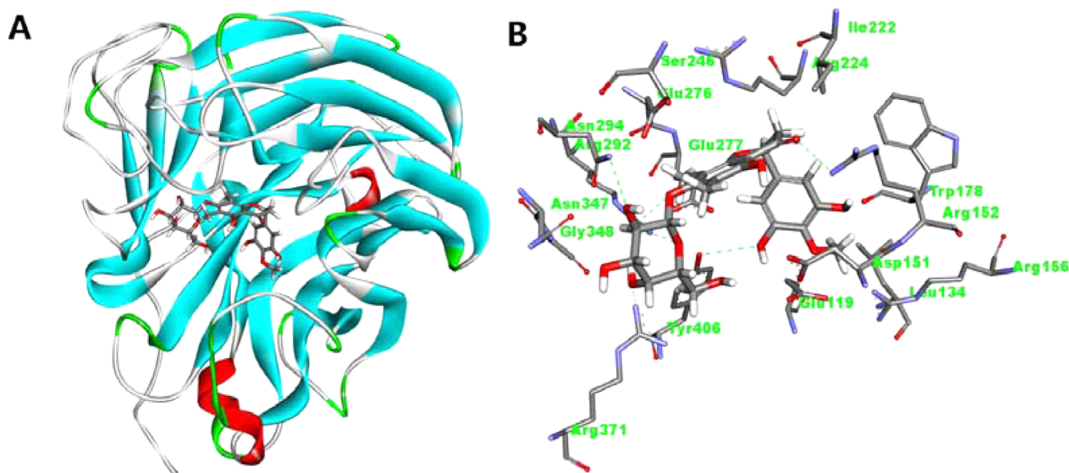
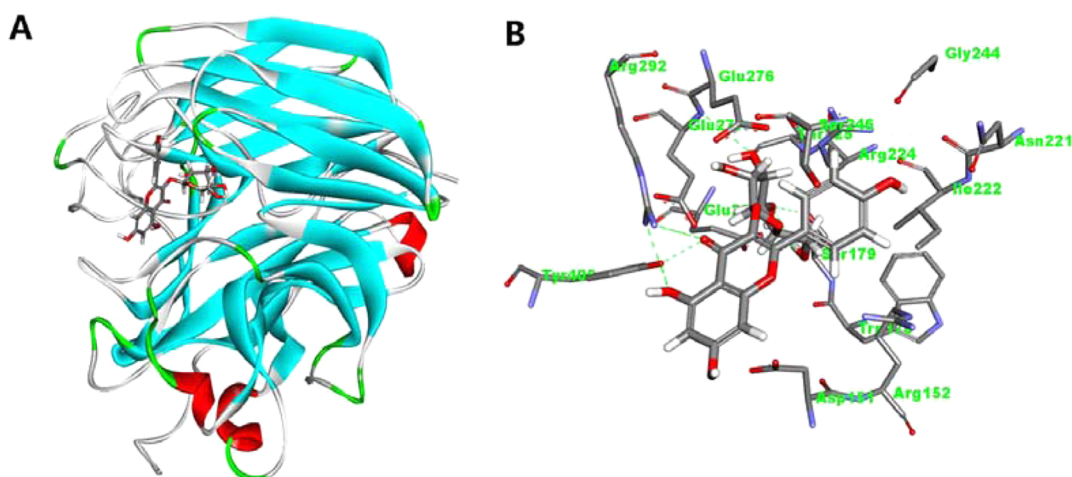
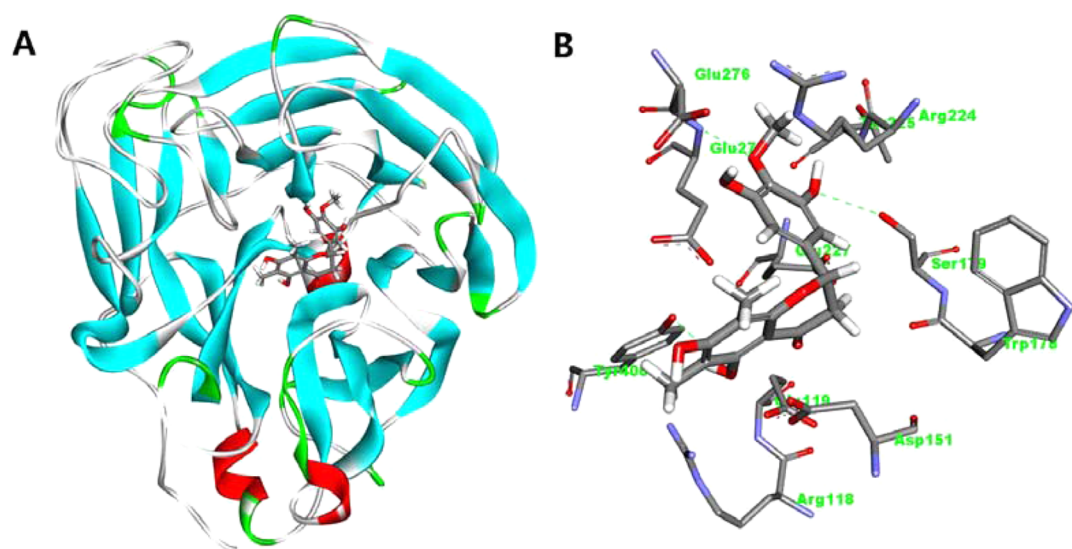


Figure 3. (A) Docked conformation of compound 7 with neuraminidase. (B) Binding modes of compound 7 with the key residues of neuraminidase that are essential for the binding.



**Figure 4.** (A) Docked conformation of compound 8 with neuraminidase. (B) Binding modes of compound 8 with the key residues of neuraminidase that are essential for the binding.



**Figure 5.** (A) Docked conformation of compound 17 with neuraminidase. (B) Binding modes of compound 17 with the key residues of neuraminidase that are essential for the binding.

All of the isolated compounds were evaluated for their anti-influenza virus (H1N1) activity using the neuraminidase inhibition assay. Cell viability was measured in parallel with the AlamarBlue assay to exclude the bioactivity resulting from the cytotoxicity of tested compounds. Ribavirin, an approved antiviral drug, was used as a positive control and showed an  $EC_{50}$  value of  $19.7 \pm 1.0 \mu\text{M}$  and a selective index (SI,  $CC_{50}/EC_{50}$ ) value greater than 10.2. Compounds 7, 8, and 17 exhibited inhibitory activity against neuraminidase from H1N1 influenza virus with  $EC_{50}$  values of  $6.8 \pm 1.1$ ,  $30.5 \pm 1.0$ , and  $72.8 \pm 1.1 \mu\text{M}$ , and SI values of 34.4, 12.4, and 3.1, respectively, while significant cytotoxicity was found for compound 16. The other tested compounds showed low cytotoxicity but were inactive in the neuraminidase inhibition assay. Therefore, matteflavoside G (7) may be a potential antiviral agent against influenza A (H1N1) on the basis of the SI value.

To further investigate the binding conformations of the active compounds to neuraminidase, molecular docking modeling was carried out using the Libdock method to dock compounds 7, 8, and 17 into the active sites of neuraminidase. The docked conformations of the best-fit ligands were

visualized: these fits extended deep into the active site pocket, forming several hydrogen bonds and hydrophobic interactions with the key residues of the active site (Figures 3–5). The docking results showed that the hydrogen bond interactions played important roles in the ligand–protein interactions. Compound 7 could form six hydrogen bonds with six residues (Trp178, Glu277, Arg292, Asn294, Arg371, and Tyr406); compound 8 could form five hydrogen bonds with four residues (Ser179, Glu277, Arg292, and Tyr406); and compound 17 could form only three hydrogen bonds with three residues (Ser179, Glu277, and Tyr406). The above molecular docking results suggested that compound 7 could combine tightly with neuraminidase, consistent with the results of the neuraminidase inhibition assay. The specific molecular mechanism needs to be clarified by further investigations.

## ■ EXPERIMENTAL SECTION

**General Experimental Procedures.** Optical rotations were measured with a JASCO P-1020 digital polarimeter ( $l = 1 \text{ cm}$ ) (JASCO, Kyoto, Japan). IR spectra (KBr disks) were obtained with a Bruker IFS-55 spectrometer (Bruker, Rheinstetten, Germany). UV

spectra were recorded on a Shimadzu UV-2201 UV-vis recording spectrophotometer (Shimadzu, Kyoto, Japan). ECD spectra were performed on a Biologic MOS-450 spectrometer (BioLogic Science Instruments, Grenoble, France). The 1D and 2D NMR spectra were obtained using Bruker AVANCE-400 or AVANCE-600 NMR spectrometers (Bruker). HRESIMS data were acquired using a Waters Synapt G2 QTOF mass spectrometer (Waters, Milford, MA, USA). The analytical HPLC was performed using an Agilent 1200 (Agilent Technologies, Santa Clara, CA, USA) equipped with a DAD detector using a reversed-phase C<sub>18</sub> column (5  $\mu$ m, 4.60  $\times$  250 mm; Phenomenex Gemini, Phenomenex Inc., Torrance, CA, USA). Semipreparative HPLC was carried out on a Shimadzu LC-6AD (Shimadzu) with a UV SPD-20A detector using a reversed-phase C<sub>18</sub> column (5  $\mu$ m, 10  $\times$  250 mm; Phenomenex Gemini, Phenomenex). Column chromatography was performed using macroporous adsorptive resins (Diaion HP20, Mitsubishi Chemical Corporation, Tokyo, Japan), silica gel (200–300 mesh, Qingdao Haiyang Chemical Co., Ltd., Qingdao, China), ODS (60–80  $\mu$ m, YMC, Tokyo, Japan), and Sephadex LH-20 (GE Healthcare Biosciences AB, Uppsala, Sweden). Silica gel G plates (Qingdao Haiyang Chemical Co., Ltd., Qingdao, China) were used for TLC analysis.

**Plant Material.** The rhizomes of *M. struthiopteris* were collected from Liaoning province, China, in September 2011, and authenticated by Professor Jin-Cai Lu, Shenyang Pharmaceutical University. A voucher specimen (YLBMS-2011) was deposited at the College of Traditional Chinese Materia Medica, Shenyang Pharmaceutical University, China.

**Extraction and Isolation.** The air-dried rhizomes (9 kg) of *M. struthiopteris* were refluxed with 60% EtOH (v/v, 2  $\times$  70 L, 2 h each). The combined extracts were concentrated in vacuo to afford a yellow residue (670 g), which was dissolved in H<sub>2</sub>O (approximately 2.7 L) and subjected to column chromatography (CC) over Diaion HP20 macroporous adsorptive resins and eluted with EtOH/H<sub>2</sub>O (0:100 to 95:5). The 95% EtOH (v/v) eluate (27 g) was subjected to column chromatography on silica gel and eluted with CH<sub>2</sub>Cl<sub>2</sub>/MeOH (100:0 to 0:100) to afford eight fractions (Fr. D1–D8). Compound **19** (11.0 mg) was crystallized in MeOH from Fr. D2 (eluted with CH<sub>2</sub>Cl<sub>2</sub>/MeOH, 99:1). Fr. D3 (eluted with CH<sub>2</sub>Cl<sub>2</sub>/MeOH, 98:2) was passed over a Sephadex LH-20 column with CH<sub>2</sub>Cl<sub>2</sub>/MeOH (1:1) as the eluent and a silica gel column and a cyclohexane/acetone stepwise gradient; it was then applied to an ODS column and eluted with MeOH/H<sub>2</sub>O. The 40% MeOH eluate yielded **17** (76.2 mg), and the 30% MeOH eluate was further purified by preparative HPLC (pHPLC) using 40% MeOH (monitored at 254 nm) as the eluent to afford **16** (12.4 mg). Fr. D5 (eluted with CH<sub>2</sub>Cl<sub>2</sub>/MeOH, 90:10) was subjected to an ODS column and eluted with a gradient of MeOH/H<sub>2</sub>O. **7** (25.8 mg), **8** (67.2 mg), **11** (57.0 mg), **12** (13.7 mg), and **13** (24.1 mg) were obtained from the 40% MeOH eluate by purification with pHPLC (MeOH–0.05% TFA, 45:55, monitored at 260 nm). Fr. D5-5 (eluted with MeOH/H<sub>2</sub>O, 60:40) was further purified by pHPLC (MeOH–0.05% TFA, 55:45, monitored at 260 nm) to afford **5** (8.5 mg) and **6** (10.3 mg). Fr. D6 (eluted with CH<sub>2</sub>Cl<sub>2</sub>/MeOH, 85:15) was applied to an ODS column eluted with a gradient of MeOH/H<sub>2</sub>O. The eluents of 40% MeOH and 50% MeOH were purified by pHPLC (45% MeOH and 50% MeOH, respectively, monitored at 260 nm) to yield **15** (39.1 mg) and **10** (20.1 mg), respectively. Fr. D7 (eluted with CH<sub>2</sub>Cl<sub>2</sub>/MeOH, 8:2/7:3) was separated by an ODS column and eluted with a gradient of MeOH/H<sub>2</sub>O. Fr. D7-3 (eluted with MeOH/H<sub>2</sub>O, 40:60) was passed over a Sephadex LH-20 column, eluted with 50% MeOH–H<sub>2</sub>O, and then further purified by pHPLC (MeOH–0.05% TFA, 40:60, monitored at 260 nm) to afford **9** (12.3 mg). Fr. D7-5 (eluted with MeOH/H<sub>2</sub>O, 50:50) was further subjected to a silica gel column and eluted with CH<sub>2</sub>Cl<sub>2</sub>/MeOH (9:1 to 7:3). Purification of Fr. D7-5-3 (eluted with CH<sub>2</sub>Cl<sub>2</sub>/MeOH, 8:2) by pHPLC (MeOH–0.05% TFA, 45:55, monitored at 260 nm) gave **3** (8.1 mg) and **4** (5.8 mg).

The 50% EtOH (v/v) eluate (20 g) from the Diaion HP20 macroporous adsorptive resin CC was subjected to column chromatography on silica gel and eluted with CH<sub>2</sub>Cl<sub>2</sub>/MeOH (100:0 to 0:100) to afford eight fractions (Fr. C1–C8). Fr. C6

(eluted with CH<sub>2</sub>Cl<sub>2</sub>/MeOH, 8:2) was subjected to an ODS column and eluted with a gradient of MeOH/H<sub>2</sub>O. Fr. C6-2 (eluted with MeOH/H<sub>2</sub>O, 30:70) was further purified by pHPLC (MeOH–0.05% TFA, 30:70, monitored at 260 nm) to afford **18** (12.5 mg). Fr. C6-3 (eluted with MeOH/H<sub>2</sub>O, 40:60) was passed over a Sephadex LH-20 column, eluted with CH<sub>2</sub>Cl<sub>2</sub>/MeOH, 1:1, and purified by pHPLC (MeOH–0.05% TFA, 37:63, monitored at 260 nm) to yield **1** (8.0 mg). Fr. C7 (eluted with CH<sub>2</sub>Cl<sub>2</sub>/MeOH, 7:3 and 1:1) was subjected to an ODS column and eluted with a gradient of MeOH/H<sub>2</sub>O. The 40% MeOH eluate was passed over a Sephadex LH-20 column, eluted with CH<sub>2</sub>Cl<sub>2</sub>/MeOH, 1:1, and purified by pHPLC (MeOH–0.05% TFA, 37:63, monitored at 260 nm) to afford **2** (11.4 mg) and **14** (20.8 mg).

**Matteflavoside A (1):** yellowish, amorphous powder;  $[\alpha]_D^{25}$  –13.4 (c 0.5, MeOH); UV (MeOH)  $\lambda_{\max}$  (log  $\epsilon$ ) 241 (4.34), 266 (4.50), 286 (4.14), 346 (4.37) nm; IR (KBr)  $\nu_{\max}$  3427, 2923, 1655, 1602, 1492, 1450, 1383, 1205, 1176, 1114, 961, 820, 621 cm<sup>-1</sup>; <sup>1</sup>H NMR (DMSO-*d*<sub>6</sub>, 400 MHz), see Table 1; <sup>13</sup>C NMR (DMSO-*d*<sub>6</sub>, 100 MHz), see Table 2; HRESIMS *m/z* 725.2296 [M + H]<sup>+</sup> (calcd for C<sub>33</sub>H<sub>41</sub>O<sub>18</sub>, 725.2293).

**Matteflavoside B (2):** yellowish, amorphous powder;  $[\alpha]_D^{25}$  –30.4 (c 0.5, MeOH); UV (MeOH)  $\lambda_{\max}$  (log  $\epsilon$ ) 241 (4.14), 266 (4.30), 286 (3.94), 346 (4.16) nm; IR (KBr)  $\nu_{\max}$  3418, 2923, 1656, 1602, 1492, 1450, 1384, 1208, 1177, 1114, 962, 821, 620 cm<sup>-1</sup>; <sup>1</sup>H NMR (DMSO-*d*<sub>6</sub>, 400 MHz), see Table 1; <sup>13</sup>C NMR (DMSO-*d*<sub>6</sub>, 100 MHz), see Table 2; HRESIMS *m/z* 741.2242 [M + H]<sup>+</sup> (calcd for C<sub>33</sub>H<sub>41</sub>O<sub>19</sub>, 741.2242).

**Matteflavoside C (3):** yellowish, amorphous powder;  $[\alpha]_D^{25}$  –70.4 (c 0.5, MeOH); UV (MeOH)  $\lambda_{\max}$  (log  $\epsilon$ ) 264 (4.12), 343 (3.96) nm; IR (KBr)  $\nu_{\max}$  3442, 2922, 1654, 1600, 1448, 1384, 1205, 1175, 1116, 620 cm<sup>-1</sup>; <sup>1</sup>H NMR (DMSO-*d*<sub>6</sub>, 400 MHz), see Table 1; <sup>13</sup>C NMR (DMSO-*d*<sub>6</sub>, 100 MHz), see Table 2; HRESIMS *m/z* 783.2366 [M + H]<sup>+</sup> (calcd for C<sub>35</sub>H<sub>43</sub>O<sub>20</sub>, 783.2348).

**Matteflavoside D (4):** yellowish, amorphous powder;  $[\alpha]_D^{25}$  –25.2 (c 0.5, MeOH); UV (MeOH)  $\lambda_{\max}$  (log  $\epsilon$ ) 227 (3.98), 264 (4.07), 342 (3.87) nm; IR (KBr)  $\nu_{\max}$  3421, 2923, 1726, 1655, 1600, 1492, 1450, 1384, 1206, 1175, 1127, 970, 840, 620 cm<sup>-1</sup>; <sup>1</sup>H NMR (DMSO-*d*<sub>6</sub>, 400 MHz), see Table 1; <sup>13</sup>C NMR (DMSO-*d*<sub>6</sub>, 100 MHz), see Table 2; HRESIMS *m/z* 783.2345 [M + H]<sup>+</sup> (calcd for C<sub>35</sub>H<sub>43</sub>O<sub>20</sub>, 783.2348).

**Matteflavoside E (5):** yellowish, amorphous powder;  $[\alpha]_D^{25}$  –79.2 (c 0.5, MeOH); UV (MeOH)  $\lambda_{\max}$  (log  $\epsilon$ ) 265 (4.17), 342 (4.02) nm; IR (KBr)  $\nu_{\max}$  3428, 2920, 1665, 1662, 1597, 1443, 1384, 1206, 1176, 1138, 840, 723, 620 cm<sup>-1</sup>; <sup>1</sup>H NMR (DMSO-*d*<sub>6</sub>, 600 MHz), see Table 1; <sup>13</sup>C NMR (DMSO-*d*<sub>6</sub>, 150 MHz), see Table 2; HRESIMS *m/z* 737.2292 [M + H]<sup>+</sup> (calcd for C<sub>34</sub>H<sub>41</sub>O<sub>18</sub>, 737.2293).

**Matteflavoside F (6):** yellowish, amorphous powder;  $[\alpha]_D^{25}$  –8.4 (c 0.5, MeOH); UV (MeOH)  $\lambda_{\max}$  (log  $\epsilon$ ) 265 (4.13), 342 (3.95) nm; IR (KBr)  $\nu_{\max}$  3428, 2925, 1741, 1660, 1600, 1449, 1384, 1206, 1176, 1137, 841, 620 cm<sup>-1</sup>; <sup>1</sup>H NMR (DMSO-*d*<sub>6</sub>, 400 MHz), see Table 1; <sup>13</sup>C NMR (DMSO-*d*<sub>6</sub>, 100 MHz), see Table 2; HRESIMS *m/z* 783.2351 [M + H]<sup>+</sup> (calcd for C<sub>35</sub>H<sub>43</sub>O<sub>20</sub>, 783.2348).

**Matteflavoside G (7):** yellowish, amorphous powder;  $[\alpha]_D^{25}$  –4.0 (c 0.5, MeOH); UV (MeOH)  $\lambda_{\max}$  (log  $\epsilon$ ) 283 (4.08), 357 (3.41) nm; ECD (c = 0.5  $\times$  10<sup>-3</sup>, MeOH)  $\Delta\epsilon$  (nm): –16.3 (282.6), 6.38 (353.6); IR (KBr)  $\nu_{\max}$  3442, 2928, 1633, 1601, 1515, 1442, 1384, 1286, 1188, 1124, 993, 891, 616 cm<sup>-1</sup>; <sup>1</sup>H NMR (DMSO-*d*<sub>6</sub>, 400 MHz), see Table 1; <sup>13</sup>C NMR (DMSO-*d*<sub>6</sub>, 100 MHz), see Table 2; HRESIMS *m/z* 509.1661 [M + H]<sup>+</sup> (calcd for C<sub>24</sub>H<sub>29</sub>O<sub>12</sub>, 509.1659).

**Acid Hydrolysis and HPLC Analysis.** The absolute configurations of the sugar moieties in the structures were determined by the method of Tanaka et al.<sup>17</sup> Compound **1** (3 mg) was hydrolyzed with 2 M HCl for 2 h at 90 °C. The mixture was evaporated to dryness in vacuo, and the residue was dissolved in H<sub>2</sub>O and extracted with CHCl<sub>3</sub>. After the aqueous layer was dried in vacuo, the residue was dissolved in pyridine (1 mL) containing L-cysteine methyl ester (1 mg) (Sigma, USA) and heated at 60 °C for 1 h. *o*-Tolyl isothiocyanate (5 mL) (Alfa Aesar, U.K.) was added, and the mixture was heated at 60 °C for 1 h and directly analyzed by HPLC. Analytical HPLC was performed on a reversed-phase C<sub>18</sub> column (5  $\mu$ m, 4.60  $\times$  250 mm;

Phenomenex Gemini) at 35 °C with isocratic elution using 25% CH<sub>3</sub>CN containing 0.1% formic acid for 40 min at a flow rate 0.8 mL/min. The peaks were detected with a UV detector at 250 nm. The standard monosaccharides, L-rhamnose, D-glucose, L-glucose, and D-galactose (Sigma, USA), were subjected to the same process. The peaks of the standard monosaccharide derivatives were recorded at  $t_R$  17.1 (D-Gal), 17.9 (L-Glc), 19.5 (D-Glc), and 32.8 (L-Rha) min. Following the above procedure, the derivatives of 1, 5, and 6 afforded one peak at  $t_R$  = 32.8 min (L-Rha), and the derivatives of 2 and 3 both gave two peaks at  $t_R$  = 17.1 (D-Gal) and 32.8 (L-Rha) min; the derivative of 4 gave two peaks at  $t_R$  = 19.5 (D-Glc) and 32.8 (L-Rha) min, and one peak of the derivative of 7 was observed at  $t_R$  = 19.5 (D-Glc) min.

**Neuraminidase Inhibition Assay.** The influenza virus strain A/PR/8/34 H1N1 was maintained and cultured in Wuhan Institute of Virology, Chinese Academy of Science. Madin-Darby canine kidney (MDCK) cells were grown in Dulbecco's modified Eagle medium (DMEM) containing 10% fetal bovine serum at 37 °C with 5% CO<sub>2</sub>.

Neuraminidase plays a key role in the release of virions from the infected host cells and in their movement through the respiratory tract,<sup>31</sup> which makes it an important target for the development of anti-influenza drugs. A fluorimetric assay was used to determine the influenza virus NA activity.<sup>32</sup> In the assay, the fluorescent product resulting from the NA-specific substrate 4-methylumbelliferyl- $\alpha$ -D-N-acetylneuraminic acid (MUNANA) catalyzed by NA was quantified, which sensitively reflects the NA activity. The reported method was adopted with some modifications.<sup>32,33</sup> MDCK cells in a 96-well microplate (2 × 10<sup>4</sup> cells/well) were infected with influenza virus (A/PR/8/34 H1N1, MOI = 0.01), and various concentrations (0.7 to 166  $\mu$ M) of the tested samples in DMEM containing 1% DMSO (dimethylsulfoxide) were added to the wells simultaneously. After being incubated at 37 °C for 1 h, the culture supernatant was removed and the virus-infected cells were washed with phosphate buffered saline. The fresh DMEM containing the tested samples at various concentrations was added to the corresponding wells. The plate was incubated at 37 °C for 48 h. The infection medium containing the tested samples (40  $\mu$ L) was transferred to a 96-well black microplate, and the substrate (20  $\mu$ L) was added to start the reaction. After incubation for 45 min at 37 °C, the reaction was terminated. The fluorescence intensity was measured with a multilabel plate reader (Wallac Envision 2102, PerkinElmer, MA, USA) (excitation 355 nm, emission 485 nm). Ribavirin at different concentrations (0.8 to 200  $\mu$ M) was used as a positive control. All tests were performed in triplicate. The inhibition ratio was determined as follows: inhibition activity (%) =  $[1 - (F_{\text{sample}} - F_{\text{cellular control}})/(F_{\text{virus}} - F_{\text{cellular control}})] \times 100\%$ , where  $F_{\text{sample}}$  is the fluorescence of the tested sample at a certain concentration,  $F_{\text{virus}}$  is the fluorescence of the influenza virus control, and  $F_{\text{cellular control}}$  is the fluorescence of normal cells. The 50% effective concentration (EC<sub>50</sub>) was determined by extrapolation of the results from various doses tested using a linear equation.

**Cytotoxicity Assay.** The AlamarBlue assay method was used to measure the cytotoxicity of the tested samples.<sup>34</sup> MDCK cells were grown in a 96-well plate (2 × 10<sup>4</sup> cells/well) for 16 h. The culture supernatant was replaced with maintenance medium containing the tested samples at various concentrations (2–500  $\mu$ M). After 72 h of incubation, the AlamarBlue (Invitrogen) solution was added to each well. The plate was incubated at 37 °C for 2 h. The fluorescence intensity, which was proportional to the number of living cells in the tested sample, was recorded with a multilabel plate reader (Wallac Envision 2102) (excitation 570 nm, emission 595 nm). The control group received an equal amount of DMSO, which resulted in a final concentration of 1% DMSO in the medium. Ribavirin at different concentrations (0.8–200  $\mu$ M) served as a positive control. All tests were performed in triplicate. The cell activity was determined as follows: cell activity (%) =  $(F_{\text{sample}} - F_{\text{blank}})/(F_{\text{cellular control}} - F_{\text{blank}}) \times 100\%$ , where  $F_{\text{sample}}$  is the fluorescence of the tested sample at a certain concentration,  $F_{\text{blank}}$  is the fluorescence of the culture medium without cell and tested samples, and  $F_{\text{cellular control}}$  is the fluorescence of normal cells without tested samples.

**Molecular Docking.** The structure building of all the compounds was performed by molecular modeling software package Discovery Studio 3.5 (Accelrys Inc., San Diego, CA, USA, 2012) and then minimized using the CharMM27 force field and the MMFF94 charge with a distance-dependent dielectric and conjugate gradient method. The optimized structures were used for all subsequent calculations. The X-ray crystal structure of the neuraminidase in complex with zanamivir was obtained from Brookhaven Protein Data Bank (entry 3B7E). The Libdock module embedded in Discovery Studio was used to dock the compounds to the binding site of neuraminidase. The active site was defined as including all atoms within a 6.5 Å radius of the cocrystallized ligand, and the default parameters were used.

## ■ ASSOCIATED CONTENT

### Supporting Information

Structures of compounds 8–19 and HRESIMS, UV, IR, and NMR spectra of compounds 1–7. The Supporting Information is available free of charge on the ACS Publications website at DOI: 10.1021/np500879t.

## ■ AUTHOR INFORMATION

### Corresponding Authors

\*X. Zhang) Tel: +86-24-23993994. Fax: +86-24-23993994. E-mail: syzalice@163.com.

\*X.-S. Yao) Tel: +86-24-23993994. Fax: +86-24-23993994. E-mail: tyaoxs@jnu.edu.cn.

### Notes

The authors declare no competing financial interest.

## ■ ACKNOWLEDGMENTS

The authors are grateful to Professor Jin-Cai Lu, Shenyang Pharmaceutical University for authentication of the plant material. Thanks are also given to the Institute of Traditional Chinese Medicine and Natural Products, Jinan University, for measuring the HRESIMS and optical rotation data. This work was supported by grants from State Key Laboratory of Bioactive Substance and Function of Natural Medicines (No. GTZK201304) and the Key Projects of the National Science and Technology Pillar Program (No. 2012BAI30B02).

## ■ REFERENCES

- (1) World Health Organization. Influenza (seasonal), Geneva Switzerland [EB/OL]. [2009-10-27]; <http://www.who.int/mediacentre/factsheets/fs211/en/index.html>.
- (2) Nguyen, P. H.; Na, M.; Dao, T. T.; Ndinteh, D. T.; Mbafor, J. T.; Park, J.; Cheong, H.; Oh, W. K. *Bioorg. Med. Chem. Lett.* **2010**, *20*, 6430–6434.
- (3) Regoes, R. R.; Bonhoeffer, S. *Science* **2006**, *312*, 389–391.
- (4) Dao, T. T.; Dang, T. T.; Nguyen, P. H.; Kim, E.; Thuong, P. T.; Oh, W. K. *Bioorg. Med. Chem. Lett.* **2012**, *22*, 3688–3692.
- (5) Pinto, L. H.; Holsinger, L. J.; Lamb, R. A. *Cell* **1992**, *69*, 517–528.
- (6) Kimberlin, D. W.; Coen, D. M.; Biron, K. K.; Cohen, J. I.; Lamb, R. A.; McKinlay, M.; Emini, E. A.; Whitley, R. J. *Antiviral Res.* **1995**, *26*, 369–401.
- (7) McKimm-Breschkin, J. L.; Selleck, P. W.; Usman, T. B.; Johnson, M. A. *Emerg. Infect. Dis.* **2007**, *13*, 1354–1357.
- (8) Schirmer, P.; Holodniy, M. *Expert Opin. Drug Saf.* **2009**, *8*, 357–371.
- (9) Flora of China Editorial Committee. *Flora Reipublicate Popularis Sinicae*; Science Publishers: Beijing; 1999; Vol. 4, pp 160–162.
- (10) Nanjing University of Chinese Medicine. *Dictionary of Traditional Chinese Herbal Medicine*, 2nd ed.; Shanghai Scientific and Technologic Publishers: Shanghai; 2006; pp 2118–2119.
- (11) Kimura, T.; Suzuki, M.; Takenaka, M.; Yamagishi, K.; Shinmoto, H. *Phytochemistry* **2004**, *65*, 423–426.

- (12) Bushway, A. A.; Serreze, D. V.; Mcgann, D. F.; True, R. H.; Work, T. M.; Bushway, R. J. *J. Food Sci.* **1985**, *50*, 1491–1492.
- (13) Zhang, D.; Li, S. B.; Yang, L.; Li, Y. J.; Zhu, X. X.; Kmoníčková, E.; Zidek, Z.; Fu, M. H.; Fang, J. *J. Asian Nat. Prod. Res.* **2013**, *15*, 1163–1167.
- (14) Yang, L.; Wang, M. Y.; Zhao, Y. Y.; Tu, Y. Y. *Zhongguozhongyaozazhi* **2004**, *29*, 647–649.
- (15) Yang, L.; Wang, M. Y.; Zhao, Y. Y.; Tu, Y. Y. *Yaouxuebao* **2005**, *40*, 252–254.
- (16) Zhang, D.; Yang, L.; Fu, M. H.; Tu, Y. Y. *Zhongguozhongyaozazhi* **2008**, *33*, 1703–1705.
- (17) Tanaka, T.; Nakashima, T.; Ueda, T.; Tomii, K.; Kouno, I. *Chem. Pharm. Bull.* **2007**, *55*, 899–901.
- (18) Nguyen, T. V. H.; Nguyen, D. T.; Nguyen, T. T.; Chau, V. M.; Phan, V. K. *Tap Chi Hoa Hoc* **2007**, *45*, 791–794.
- (19) Gaffield, W. *Tetrahedron* **1970**, *26*, 4093–4108.
- (20) Kishore, P. H.; Reddy, M. V. B.; Gunasekar, D.; Murthy, M. M.; Caux, C.; Bodo, B. *Chem. Pharm. Bull.* **2003**, *51*, 194–196.
- (21) Özden, S.; Dürüst, N.; Toki, K.; Saito, N.; Honda, T. *Phytochemistry* **1998**, *49*, 241–245.
- (22) Marzouk, M. M.; Kawashty, S. A.; Saleh, N. A. M.; Al-Nowaihi, A. S. M. *Chem. Nat. Compd.* **2009**, *45*, 483–486.
- (23) Pérez-Castorena, A. L.; Castro, A.; Romo de Vivar, A. *Phytochemistry* **1997**, *46*, 1297–1299.
- (24) Djoudi, R.; Bertrand, C.; Fiasson, K.; Comte, G.; Fenet, B.; Rabesa, Z. A. *Biochem. Syst. Ecol.* **2007**, *35*, 314–316.
- (25) Ouyang, X. L.; Fang, X. M.; Pan, Y. M.; Wei, L. X.; Wang, H. S. *Acta Chromatogr.* **2012**, *24*, 301–316.
- (26) Ibrahim, L. F.; Kawashty, S. A.; Baiuomy, A. R.; Shabana, M. M.; El-Eraky, W. I.; El-Negoumy, S. I. *Chem. Nat. Compd.* **2007**, *43*, 24–28.
- (27) Nishimura, S.; Kadode, K.; Uchida, N.; Miura, N.; Moriyama, H.; Maekawa, N. Japan Patent 2005306836, 2005.
- (28) Lin, A. S.; Chang, F. R.; Wu, C. C.; Liaw, C. C.; Wu, Y. C. *Planta Med.* **2005**, *71*, 867–870.
- (29) Oyama, K. I.; Kondo, T. *Tetrahedron* **2004**, *60*, 2025–2034.
- (30) Basnet, P.; Kadota, S.; Hase, K.; Namba, T. *Chem. Pharm. Bull.* **1995**, *43*, 1558–1564.
- (31) Dao, T. T.; Tung, B. T.; Nguyen, P. H.; Thuong, P. T.; Yoo, S. S.; Kim, E. H.; Kim, S. K.; Oh, W. K. *J. Nat. Prod.* **2010**, *73*, 1636–1642.
- (32) Potier, M.; Mameli, L.; Bélisle, M.; Dallaire, L.; Melancon, S. B. *Anal. Biochem.* **1979**, *94*, 287–296.
- (33) Bantia, S.; Ghate, A. A.; Ananth, S. L.; Babu, Y. S.; Air, G. M.; Walsh, G. M. *Antimicrob. Agents Chemother.* **1998**, *42*, 801–807.
- (34) Nociari, M. M.; Shalev, A.; Benias, P.; Russo, C. J. *Immunol. Methods* **1998**, *213*, 157–167.